

## FREQUENCY UPCONVERSION FLUORESCENCE OF Er<sup>3+</sup>-DOPED TeO<sub>2</sub>-WO<sub>3</sub> GLASS

Shilong Zhao<sup>a,\*</sup>, Xiuli Wang<sup>b</sup>, Shiqing Xu<sup>a</sup>, Lili Hu<sup>c</sup>

<sup>a</sup>College of Information Engineering, China Jiliang University, Hangzhou 310018, China

<sup>b</sup>Department of Chemistry, Hangzhou Teachers College, Hangzhou 310012, China

<sup>c</sup>Shanghai Institute of Optics and Fine Mechanics, Chinese Academy of Sciences, Shanghai 201800, China

Er<sup>3+</sup>-doped TeO<sub>2</sub>-WO<sub>3</sub> glass has been fabricated and characterized. Judd-Ofelt intensity parameters  $\Omega_t$  ( $t=2, 4, 6$ ) were calculated by absorption spectrum and Judd-Ofelt theory and found to be  $\Omega_2=5.38 \times 10^{-20} \text{ cm}^2$ ,  $\Omega_4=1.78 \times 10^{-20} \text{ cm}^2$ ,  $\Omega_6=0.75 \times 10^{-20} \text{ cm}^2$ . Intense green and weak red emission bands centered at 530 nm, 548 nm and 659 nm, corresponding to  $^2H_{11/2} \rightarrow ^4I_{15/2}$ ,  $^4S_{3/2} \rightarrow ^4I_{15/2}$  and  $^4F_{9/2} \rightarrow ^4I_{15/2}$  transitions of Er<sup>3+</sup>, were observed under 977 nm excitation. The dependence of upconversion intensities on excitation power presents two photon absorption processes for the three emission bands. The upconversion mechanism is discussed, and the dominant mechanisms are excited state absorption and energy transfer upconversion. The intense frequency upconversion fluorescence of Er<sup>3+</sup>-doped TeO<sub>2</sub>-WO<sub>3</sub> glass may be a potential material for developing upconversion fiber optical devices.

### 1. Introduction

In recent years, the upconversion fluorescence of infrared light to visible light by rare earth ions doped glasses and crystals has been investigated extensively, due to the possibility of infrared-pumped visible lasers and the potential applications in areas such as color display, optical data storage, and medical diagnostics [1–3]. Er<sup>3+</sup> ions are the most studied among rare earth ions, and the upconversion process of Er<sup>3+</sup> ion in various kinds of host materials has been investigated [4–6]. Tellurite glasses possess one of the lowest phonon energies of the oxide glasses and have a high refractive index, which enhances radiative transition in rare earth ions, making them attractive hosts for upconversion lasers. Although fluoride glasses have lower phonon energies, tellurite glasses are interesting alternatives because of their superior chemical durability, thermal stability, and mechanical strength [7]. By now, in binary tellurite glasses, the upconversion fluorescence has reported in Er<sup>3+</sup>-doped TeO<sub>2</sub>-Na<sub>2</sub>O [8], TeO<sub>2</sub>-PbO [9], TeO<sub>2</sub>-ZnO [10], and TeO<sub>2</sub>-Nb<sub>2</sub>O<sub>5</sub> [11]. Here the frequency upconversion fluorescence of Er<sup>3+</sup>-doped TeO<sub>2</sub>-WO<sub>3</sub> glass was reported.

### 2. Experimental

Glass with molar composition 75TeO<sub>2</sub>-25WO<sub>3</sub> was prepared. The Er<sup>3+</sup> doped concentration in the glass was 1.0 wt%. TeO<sub>2</sub>-WO<sub>3</sub> glass was melted using high purity raw materials in a quartz

---

\* Corresponding author. shilong\_zhao@hotmail.com

crucible at the temperature 800 °C. The melted glass was poured in a preheated steel mold and annealed at glass transition temperature. Six surfaces of the glass sample were polished to high optical quality and used for the following experiments.

The absorption spectrum of the glass sample was recorded with a PERKIN-ELMER-LANBDA 900UV/VIS/NIR spectrophotometer over a spectral range of 350–1700 nm. Frequency upconversion spectrum was obtained with a TRIAX550 spectrofluorimeter pumped by a 977 nm LD. All the measurements were taken at room temperature.

### 3. Results and discussion

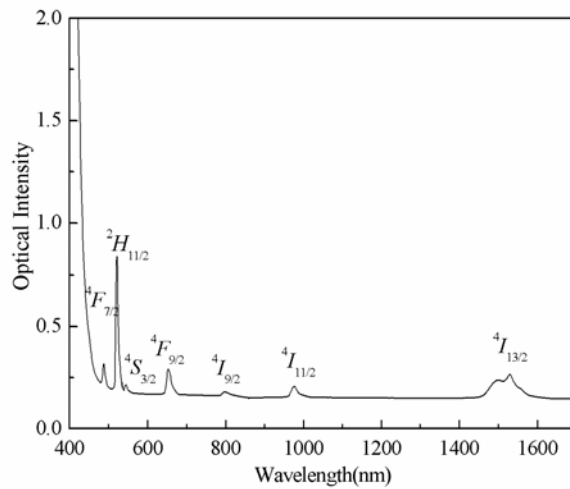


Fig. 1. Absorption spectrum of 1.0wt% Er<sup>3+</sup>-doped TeO<sub>2</sub>-WO<sub>3</sub> glass.

Fig. 1 shows the absorption spectrum of 1wt% Er<sup>3+</sup> doped TeO<sub>2</sub>-WO<sub>3</sub> glass. The band assignments are also indicated in the figure. The Judd-Ofelt parameters [12,13] were performed using the experimental oscillator strengths of the  $4f \leftrightarrow 4f$  transitions obtained from this spectrum and determined by using a least-squares fitting approach, were found to be  $\Omega_2=5.38 \times 10^{-20} \text{ cm}^2$ ,  $\Omega_4=1.78 \times 10^{-20} \text{ cm}^2$ ,  $\Omega_6=0.75 \times 10^{-20} \text{ cm}^2$ . According to previous studies [14],  $\Omega_2$  is related to the symmetry of the glass while  $\Omega_6$  is inversely proportional to covalency of the Er-O bond. As shown in Table 1, the  $\Omega_6$  in TeO<sub>2</sub>-WO<sub>3</sub> glass is smaller than those in phosphate, fluorophosphates and fluoride glasses and larger than those in germanate, silicate glasses, which indicate that covalency of the Er-O bond is higher than those in phosphate, fluorophosphates and fluoride glasses and lower than those in germanate and silicate glasses.

Table 1. Intensity parameters,  $\Omega_i$  ( $i=2, 4, 6$ ) of Er<sup>3+</sup> in various glasses.

Glass	$\Omega_2$	$\Omega_4$	$\Omega_6$
Phosphate [15]	6.65	1.52	1.11
Germanate [15]	5.81	0.85	0.28
Silicate [15]	4.23	1.04	0.61
Fluoride [15]	2.91	1.27	1.11
Fluorophosphates [16]	2.91	1.63	1.26
TeO <sub>2</sub> -WO <sub>3</sub> glass	5.38	1.78	0.75

The frequency upconversion fluorescence of TeO<sub>2</sub>-WO<sub>3</sub> glass excited at 977 nm was shown in Fig. 2. Two green emission bands centered at 530 nm and 548 nm correspond to transitions  ${}^2H_{11/2} \rightarrow {}^4I_{15/2}$  and  ${}^4S_{3/2} \rightarrow {}^4I_{15/2}$  transitions, respectively. The strong green fluorescence was observed in experiment. Weak red emission band at 659 nm corresponding to transitions  ${}^4F_{9/2} \rightarrow {}^4I_{15/2}$  also exists.

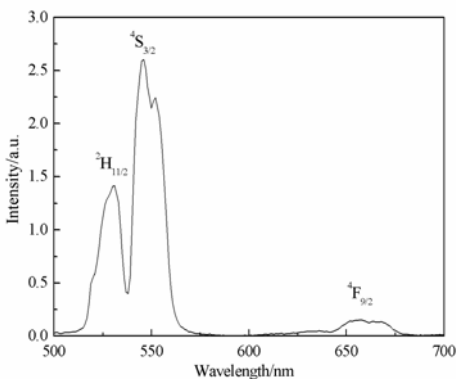


Fig. 2. Upconversion spectrum of 1.0wt% Er<sup>3+</sup>-doped TeO<sub>2</sub>-WO<sub>3</sub> glass.

In an upconversion mechanism the upconversion emission intensity  $I_{up}$  is proportional to the  $m$ th power of the infrared excitation intensity  $I_{IR}$ ; i.e.,  $I_{up} \propto I_{IR}^m$ , where  $m$  is the number of the IR photons absorbed per upconversion photon emitted. Plotting  $\log I_{UP}$  versus  $\log I_{IR}$  yields a straight line with slope  $m$ , as shown in Fig. 3 for the green and red emissions. The values of  $m$  obtained were 2.08, 1.92 and 1.77, respectively. These results indicate that a two-photon absorption contributes to the green and the red upconversion emission bands.

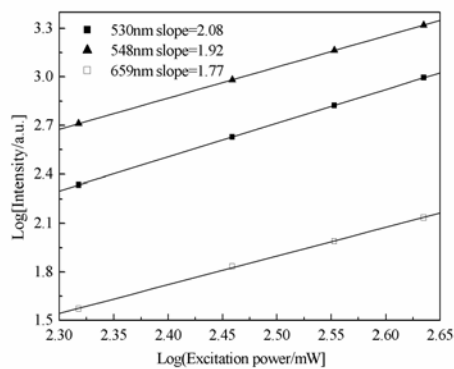


Fig. 3. Dependence of the integrated intensity of upconversion emission on excitation power.

According to the energy-matching conditions and the quadratic dependence on excitation power, the possible upconversion mechanisms for the emission bands are discussed based on the simplified energy levels of Er<sup>3+</sup> presented in Fig. 4. For the green emissions, in the first step, the  ${}^4I_{11/2}$  level is directly excited at 977 nm. The second step involves the excitation processes based on the long-lived  ${}^4I_{11/2}$  level as follows: energy transfer (ET)  ${}^4I_{11/2} + {}^4I_{11/2} \rightarrow {}^4F_{7/2} + {}^4I_{15/2}$ , and excited state absorption (ESA)  ${}^4I_{11/2} + \text{a photon} \rightarrow {}^4F_{7/2}$ . The populated  ${}^4F_{7/2}$  level Er<sup>3+</sup> then relaxes rapidly and nonradiatively to the next lower levels  ${}^2H_{11/2}$  and  ${}^4S_{3/2}$  resulting from the small energy gap between the levels. Er<sup>3+</sup> ions at the  ${}^2H_{11/2}$  state can also decay to the  ${}^4S_{3/2}$  state due to the multiphonon relaxation process. The estimated energy gap between the  ${}^2H_{11/2}$  state and the next lower state  ${}^4S_{3/2}$  is  $\sim 800 \text{ cm}^{-1}$ . Thus, multiphonon relaxation rate is very large and the 530 nm emission intensity is reduced. The above processes then produce the two  ${}^2H_{11/2} \rightarrow {}^4I_{15/2}$  and  ${}^4S_{3/2} \rightarrow {}^4I_{15/2}$  green emission, respectively. The red emission band is originated from the  ${}^4F_{9/2} \rightarrow {}^4I_{15/2}$  transition and the population of  ${}^4F_{9/2}$  are based on the processes as follows: ESA:  ${}^4I_{13/2} + \text{a photon} \rightarrow {}^4F_{9/2}$ , and ET between Er<sup>3+</sup> ions:

${}^4I_{13/2}+{}^4I_{11/2}\rightarrow{}^4F_{9/2}+{}^4I_{15/2}$ . The  ${}^4I_{13/2}$  level is populated owing to the nonradiatively relaxation from the upper  ${}^4I_{11/2}$  level. Besides, the nonradiatively process from  ${}^4S_{3/2}$  level, which is populated by means of the process described previously, to  ${}^4F_{9/2}$  level also contributes to the red emission.

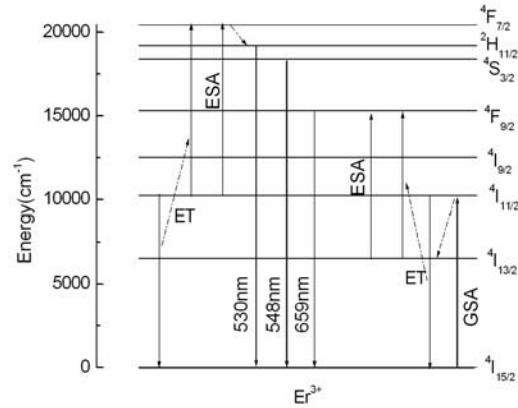


Fig. 4. Energy level diagram of Er<sup>3+</sup> ions and upconversion mechanism in Er<sup>3+</sup>-doped TeO<sub>2</sub>-WO<sub>3</sub> glass.

#### 4. Conclusions

Er<sup>3+</sup>-doped TeO<sub>2</sub>-WO<sub>3</sub> glass has been fabricated and characterized. The Judd-Ofelt intensity parameters  $\Omega_t$  ( $t=2, 4, 6$ ) were calculated by Judd-Ofelt theory. Infrared to visible upconversion fluorescence of Er<sup>3+</sup>-doped TeO<sub>2</sub>-WO<sub>3</sub> glass, excited by 977 nm LD, was reported. The frequency upconversion fluorescence of Er<sup>3+</sup>-doped TeO<sub>2</sub>-WO<sub>3</sub> glass has been investigated experimentally. Intense green and weak red emission bands centered at 530 nm, 548 nm and 659 nm, corresponding to  ${}^2H_{11/2}\rightarrow{}^4I_{15/2}$ ,  ${}^4S_{3/2}\rightarrow{}^4I_{15/2}$  and  $F_{9/2}\rightarrow{}^4I_{15/2}$  transitions of Er<sup>3+</sup>, were observed under 977 nm excitation.

#### Acknowledgements

The work was supported by the foundation of Zhejiang Provincial Education Department (No 20050394).

#### References

- [1] S. O. Man, E. Y. B. Pun, P. S. Chung, Appl. Phys. Lett. **77**, 483 (2000).
- [2] A. S. Oliverira, M. T. De Araujo, A. S. Gouveia-Neto, J. Appl. Phys. **83**, 604 (1998).
- [3] L. H. Huang, X. R. Liu, W. Xu, J. Appl. Phys. **90**, 5550 (2001).
- [4] M. Shojiya, M. Takahashi, R. Kanno, Appl. Phys. Lett. **65**, 1874 (1994).
- [5] K. Kojima, S. Yoshida, H. Shiraishi, Appl. Phys. Lett. **67**, 3423 (1995).
- [6] J. J. Ju, T. Y. Kwon, S. I. Yun, Appl. Phys. Lett. **69**, 1358 (1996).
- [7] J. S. Wang, E. M. Vogel, E. Snitzer, Opt. Mater. **3**, 187 (1994).
- [8] J. Y. Allain, M. Monerie, H. Poignant, Electron. Lett. **28**, 111 (1992).
- [9] C. Zhu, X. Lu, Z. Zhang, J. Non-Crystal. Solids **144**, 89 (1992).
- [10] J-C Boyer, F. Vetrone, J. A. Capobianco, Appl. Phys. Lett. **80**, 1752 (2002).
- [11] H. Lin, G. Meredith, S. Jiang, J. Appl. Phys. **93**, 186 (2003).
- [12] B. R. Judd, Phys. Rev. **127**, 750 (1962).
- [13] G. S. Ofelt, J. Chem. Phys. **37**, 511 (1962).
- [14] S. Tanabe, J. Non-Cryst. Solids **259**, 1 (1999).
- [15] A. R. Devi, C. K. Jaaysankar, J. Non-Cryst. Solids **197**, 111 (1996).
- [16] X. Zou, T. Izumitani, J. Non-Cryst. Solids **162**, 68 (1993).